

### 3D investigations of a radio-frequency plasma with a Langmuir Probe

S. Devaux, E. Faudot, J. Moritz, S. Heuraux

*Institut Jean Lamour, CNRS- University of Lorraine, Vandoeuvre-lès-Nancy, France*

#### Introduction

Among all the diagnostics investigating plasmas, cylindrical Langmuir probes (LP) are commonly used and are probably the simplest ones in their design, as they consist of a thin metallic wire, usually made of tungsten, inserted into the plasma. A ramp of biasing is applied to the tip of the probe, which repel or pull toward it the different species of the plasma. Meaningful pieces of information are then derived from the current measured. Difficulties arise at that stage of the process, for the interpretation of probe measurements, the so-called I-V characteristics, is among the trickiest to perform in plasma physics [1]. It indeed requires applying the proper theories about electron and ion collection, which strongly depends on the very properties of the plasma which has to be characterized. If individual tweaking is acceptable when the analysis only concerns a few of measurements, it becomes practically impossible when datasets of thousands of I-V are to be analyzed. One then wants to rationalize the steps of the process so that analysis can be automatically performed. Fortunately, probes are investigated for decades and theories describing the different plasma conditions have been the purpose of numerous publications [2-6]. For low-pressure plasmas, it is mandatory to take into account the expansion of the sheath in response to the polarisation of the probe. The problem is that this expansion depends on the sheath collisional regimes which might be uncertain. In this paper, after a brief description of the ALINE device, we give an overview of the different possible collisional sheath regimes. We then present the application of our method to an Argon plasma discharge and present 3D maps of its characteristics.



**Figure 1:** The cylindrical Langmuir probe in an Argon plasma in ALINE. The radio-frequency antenna is the disc seen in the.

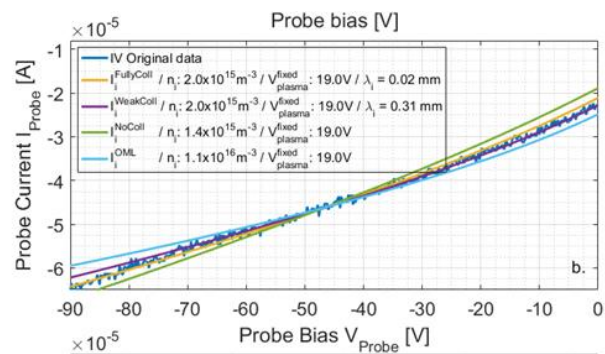


**Figure 2:** Result of the fit procedures to the ion current of a plasma. Argon pressure  $1.7 \cdot 10^{-2}$  mbar, 31.6W of input power at 35MHz.

## Experimental setup

The ALINE device [7] is a stainless steel 100cm x 30cm cylindrical vacuum chamber. Low pressure Argon plasmas are created by a capacitive RF antenna powered by a generator that can deliver up to 600W, working at frequencies between 10kHz and 250MHz. The typical neutral pressure is in the  $10^{-3} - 10^{-2}$  range. The plasma densities achieved in unmagnetized plasmas are around  $10^{14}$ - $10^{16}$  m<sup>-3</sup> for an electron temperature of a few eV [8]. The plasmas are investigated thanks to RF compensated LP [9, 10]. Its Tungsten cylindrical tip has a length of 10mm for a 0.15mm diameter. It can be biased from -200V up to 100V, which is suitable for the plasma potential usually observed around a few tens of Volts. The probe is mounted on a translatable arm, actuated by 3 steps motors, which have a positioning accuracy down to 0.1mm. The arm is fully automated thanks to a Python software. In the figure we present case, the z direction is along the axis of the machine; y the elevation above the antenna and x is perpendicular to the axis of the machine as seen on Figure 1.

## Current collection by a cylindrical Langmuir probe

Ions and electrons currents collected by the probe depend on the applied probe bias. Two values are of particular interest: the plasma potential  $V_{\text{plasma}}$  is the ones below electrons are repelled and ions attracted; the floating potential  $V_{\text{float}}$  is the potential for which ion and electron currents cancel out and no net current is drawn from the plasma.

### A. Electron current between the floating potential and the plasma potential

For a bias increasing from  $V_{\text{float}}$  to  $V_{\text{plasma}}$ , electrons are repelled by the electric field but quickly dominate the ion contribution due to their much greater thermal speed. Assuming a Maxwellian velocity distribution function and Boltzmann equilibrium for the electrons, the electron current measured by the probe is given by:

$$I_e = A_{\text{probe}} e n_e \left( \frac{k_B T_e}{2\pi m_e} \right)^{\frac{1}{2}} \exp \left( \frac{e(V_{\text{probe}} - V_{\text{plasma}})}{k_B T_e} \right) \quad (1)$$

where  $I_e$  is the electron current,  $k_B$  the Boltzmann constant,  $A_{\text{probe}}$  the probe area,  $e$ ,  $n_e$ , and  $T_e$  are the electron charge, density and temperature, respectively.  $V_{\text{probe}}$  is the probe potential.

### B. Ion current below the floating potential

For  $V_{\text{probe}} < V_{\text{float}}$ , the current is mainly the ion contribution. For low pressure and density plasmas, where the sheath length is millimetric or centimetric, the ion current is dominated by the sheath expansion due to the applied probe potential. The ion current is given by:

$$I_i = \alpha_0 n_i A_{\text{sheath}} c_s \quad (2)$$

where  $\alpha_0 \approx 0.5$  for ions at the room temperature and  $c_s$  the Bohm speed. The collection area  $A_{\text{sheath}}$  is assumed to be the sheath surface:  $A_{\text{sheath}} = 2\pi l_{\text{probe}} \times (r_{\text{probe}} + \lambda_{\text{sheath}})$ , where  $l_{\text{probe}}$  is the probe length,  $r_{\text{probe}}$  its radius and  $\lambda_{\text{sheath}}$  the sheath radial length. Here we present the three different expressions in a form suitable for a fit procedure, i.e. which emphasizes the role of the plasma parameters. One should refer to [11] for the derivation of those expressions.

For a ratio of ion mean free path to Debye length ratio  $\lambda_i/\lambda_{\text{De}} > 10$ , ions are considered collisionless. The ion motion equation is solved considering only their inertia and the electric potential well. After a few manipulations it comes:

$$\lambda_{\text{sheath}}^{\text{NoColl}} = \frac{24}{3} \times e^{-\frac{1}{4}} \epsilon_0^{\frac{1}{2}} \times \left( n_i T_e^{\frac{1}{2}} \right)^{-\frac{1}{2}} \times (V_{\text{plasma}} - V_{\text{probe}})^{\frac{3}{4}} \quad (3)$$

where  $\epsilon_0$  is the vacuum electric permittivity.

For intermediate pressure plasmas, collisions have to be taken into account. The ion mobility depends on the fluid velocity and a similar analysis as above leads to:

$$\lambda_{\text{sheath}}^{\text{WeaklyColl}} = \left( \frac{5}{3} \right)^{\frac{3}{5}} \left( \frac{8}{9\pi} \right)^{\frac{1}{5}} e^{-\frac{1}{5}} \epsilon_0^{\frac{2}{5}} \times \lambda_i^{\frac{1}{5}} \times \left( n_i T_e^{\frac{1}{2}} \right)^{-\frac{2}{5}} \times (V_{\text{plasma}} - V_{\text{probe}})^{\frac{3}{5}} \quad (4)$$

For high pressure, collisions dominate and the ion mobility is given by the ion thermal speed:

$$\lambda_{\text{sheath}}^{\text{FullyColl}} = \left( \frac{9}{8} \right)^{\frac{1}{3}} \epsilon_0^{\frac{1}{3}} \times T_i^{-\frac{1}{6}} \times \lambda_i^{\frac{1}{3}} \times (n_i T_e)^{-\frac{1}{6}} \times (V_{\text{plasma}} - V_{\text{probe}})^{\frac{2}{3}} \quad (5)$$

where  $T_i$  is the ion temperature (taken at the room temperature  $\sim 2.6 \cdot 10^{-2}$  eV).

### Example of ion current fit procedure

We here apply our method to the case of Fig.2, a I-V characteristic measured in Argon. Determinations of  $V_{\text{plasma}}$  and  $T_e$  are mandatory steps not described here. So is the determination of the ion mean free path, which is found by forcing  $n_i = n_e$  when fitting the full IV characteristic. Figure 2 shows the fit attempts of the ion current in the case of fixed plasma potential. The different dependences of the theoretical ion current with the applied probe bias are clearly seen. It appears that the weakly collisional theory is the closest to the experimental data, and gives an ion density compatible with the electron density derived from the electron fit. The fully collisional theory could also be compatible with the data but requires a much too low mean free path (expected around 1mm at this pressure). If we consider it the other way round, forcing the mean free path to be in the range of the expected one would give an ion density an order of magnitude lower than the electron density, well beyond the estimated uncertainty. The two other theories lead to a much worst agreement between the data and the fit curves, so that they are not considered as the relevant theory.

### 3D maps around the antenna

The automatization of the described method makes possible the analysis of thousands of characteristics without human intervention. As ALINE plasma are very stable in time, the plasma surrounding the antenna can be mapped. On figures 3 and 4, we present the result of such a mapping for two different sets of parameters, but only the space above the antenna is displayed. Both plasmas have been probed every 7mm, which represent each time 2000 I-V.

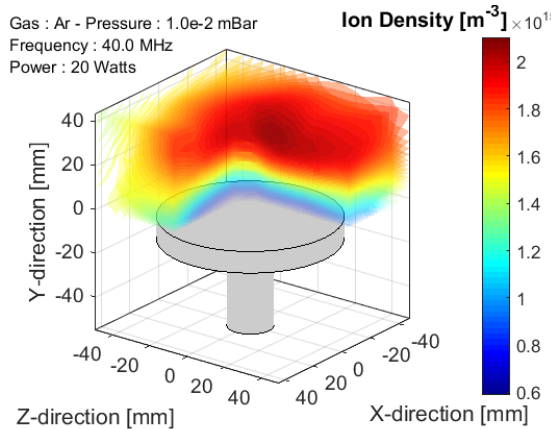


**Figure 3:** The plasma above the antenna is relatively homogenous as the high density area spread all over the antenna and beyond.

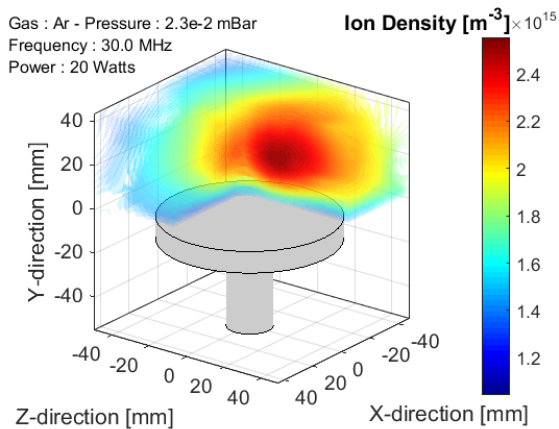


**Figure 4:** The plasma above the antenna exhibits strong gradients and the high density area is located in a bulb on top of the antenna.

Even if the two plasmas differ by the RF frequencies as well as the background pressures, they show comparable ion densities of  $2.10^{15} m^{-3}$ . The 3D mapping shows that the shapes of the plasmas are very different. At 30 MHz, the highest density is confined in a small region directly on top of the antenna, whereas high density area spread beyond the antenna in Fig.3.

### Conclusion

Thanks to the stability of ALINE plasmas and its translatable Langmuir probe, the space surrounding the RF antenna can be probed with a great accuracy. The automatization of the analysis of the IV characteristics allows for a robust derivation of the plasma parameters without human intervention. These two points open the possibility to investigate the plasma shapes above such an antenna and their modifications with the discharge input parameters.

### References

- [1] I. Cherrington, *Plasma Chemistry and Plasma Processing* **2**, (1982) 113
- [2] R.M. Clements, *J. Vac. Sci. Technol.* **15**, 193 (1978)]
- [3] I. Langmuir, *Science* **58** (1923) 290
- [4] H.M. Mott-Smith and I. Langmuir, *Phys. Rev.* **28** (1926) 727
- [5] J.E. Allen, R.L.F. Boyd and P. Reynolds., *Proc. Phys. Soc. B* **70** (1957) 297
- [6] F.F. Chen, C. Etievant, and D. Mosher, *Phys. Fluids* **2** (1959) 112
- [7] E. Faudot *et al.*, *Review of Scientific Instruments* **86** (2015) 063502
- [8] S. Devaux, E. Faudot, J. Moritz and S. Heuraux, submitted to *Nuclear Materials and Energy*
- [9] F.F. Chen, *Plasma Sources Sci. Technol.* **15** (2006) 773
- [10] P.A. Chatterton, J.A. Rees, W.L. Wu and K. Al-Assadi, *Vacuum* **42** 7 (1991) 489
- [11] P. Chabert and N. Braithwaite, *Physics of Radio-Frequency Plasmas*, Cambridge Univ. Press (2011)